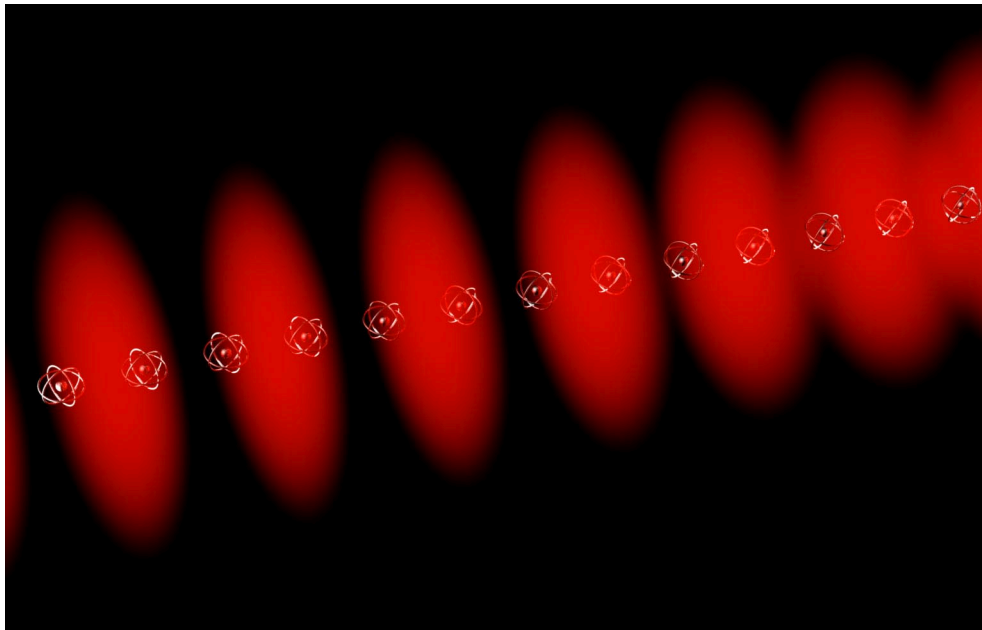# Chapter 2

Atomic Motion in an Optical Standing Wave

2.1 Overview

In this chapter we will motivate the experiments in this dissertation by considering the basic setup common to all of the experiments: the motion of an atom in a standing wave of far-detuned light. The basic conclusion of this chapter is that under the proper conditions, it is possible to ignore the internal electronic structure of the atom, and treat the atom as a point particle. Furthermore, the "reduced" atom moves under the influence of the effective center-of-mass Hamiltonian

$$H_{\text{eff}} = \frac{p^2}{2m} + V_0 \cos(2k_{\text{L}}x) , \tag{2.1}$$

where m is the atomic mass, k_{L} is the wave number of the laser light, and the potential amplitude V_0 is proportional to the laser intensity and inversely proportional to the detuning from the nearest atomic resonance (which in these experiments is one of the components of the cesium D_2 spectral line). This Hamiltonian is familiar, as it is formally equivalent to the plane-pendulum Hamiltonian. This motion is, of course, integrable, but this is nevertheless an important starting point for the realization of nonintegrable systems, as both the amplitude and phase of the potential can be modulated to realize a variety of $1\frac{1}{2}$-degree-of-freedom systems.

We begin the analysis in Section 2.2, where we set up the problem of a two-level atom interacting with a laser field. We then examine the dynamical equations of motion for the atom and derive the atomic energy shift due to the field in Section 2.3. The adiabatic approximation, which is necessary to decouple the internal and external dynamics (and thus ignore the internal degrees of freedom), is reviewed in Section 2.4. In Section 2.5 we look at the deviations that can occur from the idealized picture represented by Eq. (2.1), such as several dissipative processes as well as the treatment of cesium (which has quite a complicated hyperfine level structure) as a two-level atom. We also estimate the magnitudes of these corrections for the experiments in this dissertation. Section 2.6 covers the more general case of when the two beams that form the optical lattice differ in amplitude and frequency. We will see that the former difference can be taken into account by using the geometric mean of the two intensities as a replacement for the intensity in the identical-beam case, and the frequency difference is equivalent to a nonzero velocity of the lattice. Finally, in Section 2.7, we examine some aspects of quantum motion in

an optical lattice that will be important considerations for the experiments described in later chapters. Specifically, we will examine the how the momentum excitations due to the lattice are quantized in multiples of two photon recoil momenta ($2\hbar k_\mathrm{L}$) and how this quantization gives rise to Bragg scattering; we will also consider the band structure of the lattice, which is important in using a lattice for quantum-state preparation; and we examine the consequence of the lattice being an extended system, as opposed to a "true" pendulum that obeys periodic boundary conditions over one period of the potential.

2.2   Atom-Field Interaction

We begin our treatment with a general description of the atom-field interaction. We consider the one-dimensional problem of a two-level atom moving in a standing wave of light. The standing wave is described by the sum of two traveling waves,

$$
\begin{aligned}
\mathbf{E}(x,t) &= \hat{z}E_0[\cos(k_\mathrm{L}x - \omega_\mathrm{L}t) + \cos(k_\mathrm{L}x + \omega_\mathrm{L}t)] \\
&= \hat{z}E_0\cos(k_\mathrm{L}x)\left(e^{-i\omega_\mathrm{L}t} + e^{i\omega_\mathrm{L}t}\right) \\
&=: \mathbf{E}^{(+)}(x,t) + \mathbf{E}^{(-)}(x,t)\ ,
\end{aligned}
\tag{2.2}
$$

where $\mathbf{E}^{(+)}$ and $\mathbf{E}^{(-)}$ are the positive- and negative-rotating components of the field, respectively (i.e., $\mathbf{E}^{(\pm)} \sim e^{-i(\pm\omega_\mathrm{L})t}$), E_0 is the amplitude of either one of the two constituent traveling waves, and ω_L is the laser frequency.

The atomic free-evolution Hamiltonian is then given by

$$
H_\mathrm{A} = \frac{p^2}{2m} + \hbar\omega_0|\mathrm{e}\rangle\langle\mathrm{e}|\ ,
\tag{2.3}
$$

where the excited and ground internal atomic states are $|\mathrm{e}\rangle$ and $|\mathrm{g}\rangle$, respectively, and ω_0 is the frequency of the atomic resonance. The atom-field interaction Hamiltonian is given (in the dipole approximation) by

$$
H_\mathrm{AF} = -\mathbf{d}\cdot\mathbf{E}\ ,
\tag{2.4}
$$

where $\mathbf{d}$ is the atomic dipole operator. Assuming that $|\omega_\mathrm{L} - \omega_0| \ll \omega_\mathrm{L} + \omega_0$, we can make the rotating-wave approximation (RWA), where terms rotating at twice the optical frequencies are

replaced by their zero average value, with the result

$$
\begin{aligned}
H_{\mathrm{AF}} &= -\mathbf{d}^{(+)} \cdot \mathbf{E}^{(-)} - \mathbf{d}^{(-)} \cdot \mathbf{E}^{(+)} \\
&= -d_z^{(+)} E^{(-)} - d_z^{(-)} E^{(+)} \quad ,
\end{aligned}
\tag{2.5}
$$

where we have decomposed the dipole operator into its positive- and negative-frequency parts,

$$
\begin{aligned}
\mathbf{d} &= \mathbf{d}^{(+)} + \mathbf{d}^{(-)} \\
&= (a + a^{\dagger}) \langle e | \mathbf{d} | g \rangle \quad ,
\end{aligned}
\tag{2.6}
$$

$a := |g\rangle\langle e|$ is the atomic lowering operator, and we have taken the dipole matrix element $\langle e | \mathbf{d} | g \rangle$ to be real. We can also write the interaction Hamiltonian as

$$
H_{\mathrm{AF}} = \frac{\hbar\Omega}{2} (a e^{i\omega_{\mathrm{L}} t} + a^{\dagger} e^{-i\omega_{\mathrm{L}} t}) \cos k_{\mathrm{L}} x \quad ,
\tag{2.7}
$$

where we have defined

$$
\Omega := -\frac{2 \langle e | d_z | g \rangle E_0}{\hbar}
\tag{2.8}
$$

as the maximum Rabi frequency.

Before writing down the evolution equations, we make a transformation into the rotating frame of the laser field by defining the slowly varying excited state

$$
|\tilde{e}\rangle := e^{i\omega_{\mathrm{L}} t} |e\rangle
\tag{2.9}
$$

and the stationary field amplitudes

$$
\tilde{E}^{(\pm)} := e^{\pm i\omega_{\mathrm{L}} t} E^{(\pm)} \quad .
\tag{2.10}
$$

We can then rewrite the interaction Hamiltonian as

$$
\begin{aligned}
\tilde{H}_{\mathrm{AF}} &= -\tilde{\mathbf{d}}^{(+)} \cdot \tilde{\mathbf{E}}^{(-)} - \tilde{\mathbf{d}}^{(-)} \cdot \tilde{\mathbf{E}}^{(+)} \\
&= \frac{\hbar\Omega}{2} (\tilde{a} + \tilde{a}^{\dagger}) \cos k_{\mathrm{L}} x \quad ,
\end{aligned}
\tag{2.11}
$$

where $\tilde{\mathbf{d}}^{(\pm)}$ and $\tilde{a}$ are defined as $\mathbf{d}^{(\pm)}$ and a were defined, but with $|e\rangle$ replaced by $|\tilde{e}\rangle$. In making the rotating-wave approximation, we have discarded the two terms that would have an explicit time dependence of $e^{\pm i 2\omega_{\mathrm{L}} t}$ in Eq. (2.11), and in fact we have removed all of the explicit time dependence from this problem. Notice also that $|\tilde{e}\rangle$ is additionally an eigenstate of the internal

part of H_{A}, with eigenvalue $\hbar\omega_0 - \hbar\omega_{\mathrm{L}}$. Hence, in terms of the rotating frame excited state, the free atomic Hamiltonian becomes

$$\tilde{H}_{\mathrm{A}} = \frac{p^2}{2m} - \hbar\Delta_{\mathrm{L}}|\tilde{\mathrm{e}}\rangle\langle\tilde{\mathrm{e}}| \quad , \tag{2.12}$$

where $\Delta_{\mathrm{L}} := \omega_{\mathrm{L}} - \omega_0$ is the detuning of the laser from the atomic resonance. Again, this representation of the problem in the laser frame is interesting, because it shows that this *ac* interaction is equivalent to the problem of two states separated in energy by $\hbar\Delta_{\mathrm{L}}$ interacting with a *dc* electric field (after invoking the RWA).

2.2.1 Digression: Unitary Transformations and Field Operators

The result (2.12) also follows from formally applying the unitary transformation

$$U = \exp\left(i\omega_{\mathrm{L}}t|\mathrm{e}\rangle\langle\mathrm{e}|\right) \quad , \tag{2.13}$$

so that $|\tilde{\mathrm{e}}\rangle = U|\mathrm{e}\rangle$ (and $|\tilde{\mathrm{g}}\rangle = U|\mathrm{g}\rangle = |\mathrm{g}\rangle$), and then using the transformation law for a Hamiltonian under a time-dependent, unitary transformation [Madison98b]:

$$\tilde{H} = UHU^{\dagger} + i\hbar(\partial_t U)U^{\dagger} \quad . \tag{2.14}$$

However, this transformation does not correctly reproduce the rotating-frame interaction Hamiltonian (2.11). The problem lies in the fact that we have ignored the operator nature of the electric field. We can write the (single-mode) laser field as [Dalibard85]

$$\mathbf{E}^{(+)}(x,t) = \hat{z}\mathcal{E}\, a_{\mathrm{F}}\cos(k_{\mathrm{L}}x)\, e^{-i\omega_{\mathrm{L}}t} \quad , \tag{2.15}$$

where a_{F} is the annihilation operator for the laser field,

$$a_{\mathrm{F}} = \sum_{n=1}^{\infty}|n-1\rangle\langle n|\sqrt{n} \quad , \tag{2.16}$$

and $\mathcal{E}$ is a constant that can be written in terms of the mode volume of the field and the photon energy [Scully97]. In terms of the quantized field, the combined Hamiltonian corresponding to (2.3) and (2.4) becomes

$$\begin{aligned} H &= H_{\mathrm{A}} + H_{\mathrm{AF}} \\ &= \frac{p^2}{2m} + \hbar\omega_0|\mathrm{e}\rangle\langle\mathrm{e}| + \frac{\hbar g}{2}\left(a a_{\mathrm{F}}^{\dagger}e^{i\omega_{\mathrm{L}}t} + a^{\dagger}a_{\mathrm{F}}e^{-i\omega_{\mathrm{L}}t}\right)\cos k_{\mathrm{L}}x \quad , \end{aligned} \tag{2.17}$$

where $g := -2\langle e|d_z|g\rangle\mathcal{E}/\hbar$. This Hamiltonian is in the interaction picture with respect to the field evolution [Loudon83], because the field operators carry the explicit time dependence of the field (written out explicitly here). Thus, in addition to the transformation (2.13), we transform out of the interaction picture by applying the second transformation

$$U_{\text{I}} = \exp\left(iH_{\text{F}}t/\hbar\right) \quad , \tag{2.18}$$

where H_{F} is the field Hamiltonian, given by

$$H_{\text{F}} = \hbar\omega_{\text{L}}\left(a_{\text{F}}^{\dagger}a_{\text{F}} + \frac{1}{2}\right) \quad . \tag{2.19}$$

The resulting Hamiltonian is

$$\begin{aligned}
\tilde{H} &= \frac{p^2}{2m} + \hbar\omega_0|\tilde{e}\rangle\langle\tilde{e}| + \frac{\hbar g}{2}\left(\tilde{a}\tilde{a}_{\text{F}}^{\dagger} + \tilde{a}^{\dagger}\tilde{a}_{\text{F}}\right)\cos k_{\text{L}}x + \hbar\omega_{\text{L}}\left(\tilde{a}_{\text{F}}^{\dagger}\tilde{a}_{\text{F}} + \frac{1}{2}\right) \\
&= \tilde{H}_{\text{A}} + \tilde{H}_{\text{AF}} + \tilde{H}_{\text{F}} \quad ,
\end{aligned} \tag{2.20}$$

where the tildes indicate operators after transformation. This Hamiltonian is then in the Schrödinger picture with respect to the field, where the field time dependence is generated by the presence of H_{F}. In the classical limit, the average photon number N of the laser field is very large, and in a coherent state the fractional uncertainty in N becomes vanishingly small. Hence, the field operators a_{F} can be replaced by $\sqrt{N}$, and the field Hamiltonian reduces to a constant energy offset (and thus can be neglected). Upon making the identification $\Omega = g\sqrt{N}$, we also recover the correct form for the rotating interaction Hamiltonian (2.11). Hence we have shown that the transformations (2.9) and (2.10) arise formally from different representations of the quantized field.

With the expression (2.15) for the field operator in hand, we make one final remark about the RWA. Since $\mathbf{E}^{(+)}$ annihilates a photon from the laser field, the terms left in Eq. (2.5) correspond to raising the atomic state while lowering the field state ($d_z^{(-)}E^{(+)}$) and lowering the atomic state while raising the field state ($d_z^{(+)}E^{(-)}$). Invoking the RWA, then, amounts to keeping only the energy-conserving (resonant) terms in the interaction Hamiltonian.

2.3   Schrödinger Equation

Since we assume that the detuning from resonance is large (i.e., $\Delta_L \gg \Gamma$, where $1/\Gamma$ is the natural lifetime of $|e\rangle$), we will neglect spontaneous emission and use the Schrödinger equation,

$$(\tilde{H}_A + \tilde{H}_{AF})|\psi\rangle = i\hbar\partial_t|\psi\rangle \ , \tag{2.21}$$

to describe the atomic evolution. It is convenient to decompose the state vector $|\psi\rangle$ into a product of internal and external states,

$$|\psi\rangle = |\psi_e(t)\rangle\,|\tilde{e}\rangle + |\psi_g(t)\rangle\,|g\rangle \tag{2.22}$$

where the $|\psi_i(t)\rangle$ are states in the center-of-mass space of the atom. In the following, we will associate all time dependence of the atomic state with the center-of-mass components of the state vector. Defining the coefficients $\psi_i(x,t) := \langle x|\psi_i(t)\rangle$, the equation of motion for the wave function $\langle x|\psi\rangle$ becomes

$$i\hbar(\partial_t\psi_e|\tilde{e}\rangle + \partial_t\psi_g|g\rangle) = \\ \frac{p^2}{2m}(\psi_e|\tilde{e}\rangle + \psi_g|g\rangle) - \hbar\Delta_L\psi_e|\tilde{e}\rangle + \frac{\hbar\Omega}{2}(\psi_e|g\rangle + \psi_g|\tilde{e}\rangle)\cos k_L x \ . \tag{2.23}$$

Separating the coefficients of $|\tilde{e}\rangle$ and $|g\rangle$, we obtain the coupled pair of equations

$$i\hbar\partial_t\psi_e = \frac{p^2}{2m}\psi_e + \left(\frac{\hbar\Omega}{2}\cos k_L x\right)\psi_g - \hbar\Delta_L\psi_e \\ i\hbar\partial_t\psi_g = \frac{p^2}{2m}\psi_g + \left(\frac{\hbar\Omega}{2}\cos k_L x\right)\psi_e \ . \tag{2.24}$$

for the wave functions $\psi_i(x,t)$.

At this point we mention that it is possible to find energy eigenstates of the coupled atom-field system. From (2.24), we can find the new (internal) eigenstates by diagonalizing the matrix

$$\begin{pmatrix} -\hbar\Delta_L & \frac{\hbar\Omega}{2}\cos k_L x \\ \frac{\hbar\Omega}{2}\cos k_L x & 0 \end{pmatrix} \ , \tag{2.25}$$

where we have ignored the center-of-mass contributions to the Hamiltonian. The eigenvalues are given by

$$E_{1,2} = -\frac{\hbar\Delta_L}{2} \pm \frac{\hbar}{2}\sqrt{\Delta_L^2 + \Omega^2\cos^2 k_L x} \ , \tag{2.26}$$

with corresponding eigenvectors [Cohen-Tannoudji92; Meystre96]

$$|1\rangle = \sin\theta|g\rangle + \cos\theta|\tilde{e}\rangle$$
$$|2\rangle = \cos\theta|g\rangle - \sin\theta|\tilde{e}\rangle \quad . \tag{2.27}$$

By convention the state $|1\rangle$ has the higher energy, and the angle θ is defined via

$$\tan 2\theta = -\frac{\Omega \cos k_{\mathrm{L}}x}{\Delta_{\mathrm{L}}} \quad \left(0 \le \theta < \frac{\pi}{2}\right) \quad . \tag{2.28}$$

These states are known as the *dressed states* of the atom, and we see from Eq. (2.26) that the coupling to the field causes an avoided crossing in the energy level structure of the atom. For $\Delta_{\mathrm{L}} \gg \Omega$, we can expand the dressed-state energies (2.26), with the result

$$E_{1,2} = -\frac{\hbar\Delta_{\mathrm{L}}}{2} \pm \frac{\hbar\Delta_{\mathrm{L}}}{2} \pm \frac{\hbar\Omega^2}{4\Delta_{\mathrm{L}}} \cos^2 k_{\mathrm{L}}x + O\left(\frac{\Omega^4}{\Delta_{\mathrm{L}}^3}\right) \quad . \tag{2.29}$$

In this limit, the atom is essentially in only one of the dressed states, and so it is clear that the atom experiences an energy shift that depends sinusoidally on position. This shift in the energy levels is the *ac Stark shift*, and we will treat this phenomenon more precisely and directly in the next section, in the limit of large Δ_{L}.

2.4   Adiabatic Approximation

The equations of motion (2.24) can be greatly simplified by using the *adiabatic approximation*. We can motivate this approximation by examining the various time scales in the evolution of ψ_{e} and ψ_{g}. The kinetic-energy terms in Eqs. (2.24) induce variations on a time scale corresponding to several recoil frequencies $\omega_{\mathrm{r}} := \hbar k_{\mathrm{L}}^2/2m$, where $\omega_{\mathrm{r}} = 2\pi \cdot 2.07$ kHz for cesium. However, the pump-field terms induce motion on a time scale corresponding to the Rabi frequency (typically from zero to several hundred MHz), and the free evolution term induces motion of ψ_{e} on a time scale corresponding to Δ_{L} (typically several to many GHz); together, these terms induce internal atomic oscillations at the *generalized Rabi frequency* $\Omega_{\mathrm{gen}}(x) := \sqrt{\Omega^2 \cos^2 k_{\mathrm{L}}x + \Delta_{\mathrm{L}}^2} \simeq \Delta_{\mathrm{L}}$. Furthermore, in between these long and short time scales of external and internal atomic motion lies the damping time scale due to coupling with the vacuum, which corresponds to the natural decay rate Γ (for cesium, $\Gamma/2\pi = 5.2$ MHz). Because we are primarily interested in the slow center-of-mass atomic motion, and the internal atomic motion takes place for times much shorter

than the damping time, it is a good approximation to assume that the internal motion is damped instantaneously to equilibrium (i.e., $\partial_t \psi_e = 0$, because ψ_e is the variable that carries the natural internal free-evolution time dependence at frequency Δ_L, whereas ψ_g has no natural internal oscillation, because the state $|g\rangle$ is at zero energy). This approximation then gives a relation between ψ_e and ψ_g:

$$\left(\hbar\Delta_L - \frac{p^2}{2m}\right)\psi_e = \left(\frac{\hbar\Omega}{2}\cos k_L x\right)\psi_g \quad . \tag{2.30}$$

We can then use this constraint to eliminate ψ_e in the second of Eqs. (2.24), with the result

$$i\hbar\partial_t\psi_g = \left(\frac{p^2}{2m}\right)\psi_g + \left(\frac{\hbar\Omega^2}{4\left(\Delta_L - \frac{p^2}{2m\hbar}\right)}\cos^2 k_L x\right)\psi_g \quad . \tag{2.31}$$

We have already assumed that $\hbar\Delta_L \gg p^2/2m$, so we can ignore the momentum contribution to the cosine amplitude, and this equation becomes

$$i\hbar\partial_t\psi_g = \left(\frac{p^2}{2m}\right)\psi_g + V_0\cos(2k_L x)\psi_g \quad , \tag{2.32}$$

where we have shifted the zero of the potential energy, and

$$\begin{aligned} V_0 &:= \frac{\hbar\Omega^2}{8\Delta_L} \\ &= \frac{|\langle e|d_z|g\rangle|^2 E_0^2}{2\hbar\Delta_L} \quad . \end{aligned} \tag{2.33}$$

Since the detuning is large, nearly all the population is contained in $|g\rangle$, so the excited state completely drops out of the problem. Hence, the atom obeys the Schrödinger equation with the center-of-mass Hamiltonian

$$H = \frac{p^2}{2m} + V_0\cos(2k_L x) \quad , \tag{2.34}$$

and the atom behaves like a point particle in a sinusoidal potential, where the strength of the potential is given by (2.33). From Eq. (2.31), we see that the atomic momentum leads to a very small correction to the well depth V_0.

2.4.1 Master Equation Approach

It is also instructive to make the adiabatic approximation from the viewpoint of a master equation, where we can more explicitly see the effects of damping on the atomic motion. The master

equation for the atomic evolution (i.e., the optical Bloch equations generalized to include center-of-mass motion) has the general form [Cohen-Tannoudji77]

$$\partial_t \tilde{\rho}(t) = -\frac{i}{\hbar}[\tilde{H}_{\mathrm{A}} + \tilde{H}_{\mathrm{AF}}, \tilde{\rho}(t)] + V_{\mathrm{diss}}\tilde{\rho}(t) \qquad (2.35)$$

in the rotating basis, where the density operator is given by $\tilde{\rho} := |\psi\rangle\langle\psi|$, with $|\psi\rangle$ as in (2.22). In this equation, the commutator describes the Hamiltonian evolution of the system, and the dissipation operator V_{diss} describes spontaneous emission. We can write out the effect of the dissipation operator more explicitly, with the result [Dum92]

$$\begin{aligned}
\partial_t \tilde{\rho}(t) = & -\frac{i}{\hbar}(\tilde{H}_{\mathrm{eff}}\tilde{\rho}(t) - \tilde{\rho}(t)\tilde{H}_{\mathrm{eff}}^{\dagger}) \\
& + \Gamma \int d\Omega f_{\mathrm{sc}}(\theta, \phi) e^{ik_{\mathrm{L}}x\sin\theta\cos\phi} a\rho a^{\dagger} e^{-ik_{\mathrm{L}}x\sin\theta\cos\phi} \quad,
\end{aligned} \qquad (2.36)$$

where the effective, non-Hermitian Hamiltonian is given by

$$\tilde{H}_{\mathrm{eff}} = \tilde{H}_{\mathrm{A}} + \tilde{H}_{\mathrm{AF}} - i\frac{\hbar\Gamma}{2}|\tilde{\mathrm{e}}\rangle\langle\tilde{\mathrm{e}}| \quad, \qquad (2.37)$$

$f_{\mathrm{sc}}(\theta, \phi)$ is the angular distribution of the scattered light, and $e^{ik_{\mathrm{L}}x\sin\theta\cos\phi}$ is the momentum-shift operator (projected along the x-axis) that describes the photon recoil of the atom as it returns to the ground state. Note that in writing down (2.37), we have assumed purely radiative damping. The non-Hermitian nature of this effective Hamiltonian accounts for the damping in the system, and causes the total population to decay; the ground-state creation term (the last term in (2.36)) returns the lost population to the ground state. We can then write out the equations for the density matrix elements $\tilde{\rho}_{ij}(x, x', t) := \langle x|\langle i|\tilde{\rho}|j\rangle|x'\rangle$ as

$$\begin{aligned}
\partial_t \tilde{\rho}_{\mathrm{gg}} = & -\frac{i}{\hbar}\left[\frac{p^2}{2m}, \tilde{\rho}_{\mathrm{gg}}\right] - \frac{i\Omega}{2}\left(\cos k_{\mathrm{L}}x\tilde{\rho}_{\mathrm{eg}} - \tilde{\rho}_{\mathrm{ge}}\cos k_{\mathrm{L}}x\right) \\
& \qquad\qquad + \Gamma \int d\Omega f_{\mathrm{sc}}(\theta, \phi) e^{ik_{\mathrm{L}}x\sin\theta\cos\phi}\tilde{\rho}_{\mathrm{ee}}e^{-ik_{\mathrm{L}}x\sin\theta\cos\phi} \\
\partial_t \tilde{\rho}_{\mathrm{ee}} = & -\frac{i}{\hbar}\left[\frac{p^2}{2m}, \tilde{\rho}_{\mathrm{ee}}\right] + \frac{i\Omega}{2}\left(\cos k_{\mathrm{L}}x\tilde{\rho}_{\mathrm{eg}} - \tilde{\rho}_{\mathrm{ge}}\cos k_{\mathrm{L}}x\right) - \Gamma\tilde{\rho}_{\mathrm{ee}} \\
\partial_t \tilde{\rho}_{\mathrm{ge}} = & -\frac{i}{\hbar}\left[\frac{p^2}{2m}, \tilde{\rho}_{\mathrm{ge}}\right] - \left(\frac{\Gamma}{2} + i\Delta_{\mathrm{L}}\right)\tilde{\rho}_{\mathrm{ge}} - \frac{i\Omega}{2}\left(\cos k_{\mathrm{L}}x\tilde{\rho}_{\mathrm{ee}} - \tilde{\rho}_{\mathrm{gg}}\cos k_{\mathrm{L}}x\right) \\
\partial_t \tilde{\rho}_{\mathrm{eg}} = & -\frac{i}{\hbar}\left[\frac{p^2}{2m}, \tilde{\rho}_{\mathrm{eg}}\right] - \left(\frac{\Gamma}{2} - i\Delta_{\mathrm{L}}\right)\tilde{\rho}_{\mathrm{eg}} - \frac{i\Omega}{2}\left(\cos k_{\mathrm{L}}x\tilde{\rho}_{\mathrm{gg}} - \tilde{\rho}_{\mathrm{ee}}\cos k_{\mathrm{L}}x\right) \quad.
\end{aligned} \qquad (2.38)$$

We again assume that $\Delta_{\mathrm{L}} \gg \Gamma$ and note that the equations have fast internal driving terms (with frequencies comparable to or greater than Γ) and slow center-of-mass terms; this time, however, the equations of motion for the coherences (which are responsible for the population oscillations) have explicit damping terms. Since we are interested in the slow external motion, we can use the fact that the steady-state solution for $\tilde{\rho}_{\mathrm{ee}}$ is of order $(\Gamma/\Delta_{\mathrm{L}})^2$, whereas the steady state solutions for the coherences $\tilde{\rho}_{\mathrm{eg}}$ and $\tilde{\rho}_{\mathrm{ge}}$ are of order $\Gamma/\Delta_{\mathrm{L}}$ [Loudon83], so that we can neglect the $\tilde{\rho}_{\mathrm{ee}}$ terms on the right-hand sides of these equations. Now, we will assume that the quickly rotating coherences are damped to equilibrium on a time scale short compared to the external motion of interest, and hence set $\partial_t \tilde{\rho}_{\mathrm{ge}} = \partial_t \tilde{\rho}_{\mathrm{eg}} = 0$. Doing so leads to the adiabatic relations

$$
\begin{aligned}
\tilde{\rho}_{\mathrm{ge}} &= \frac{\Omega}{2\Delta_{\mathrm{L}}} \tilde{\rho}_{\mathrm{gg}} \cos k_{\mathrm{L}} x \\
\tilde{\rho}_{\mathrm{eg}} &= \frac{\Omega}{2\Delta_{\mathrm{L}}} \cos k_{\mathrm{L}} x \tilde{\rho}_{\mathrm{gg}} \quad,
\end{aligned}
\tag{2.39}
$$

where we have neglected the momentum and Γ terms in comparison to the Δ_{L} term. Substituting Eqs. (2.39) into the equation of motion for $\tilde{\rho}_{\mathrm{gg}}$ (and neglecting the $\tilde{\rho}_{\mathrm{ee}}$ term), we find

$$
\partial_t \tilde{\rho}_{\mathrm{gg}} = -\frac{i}{\hbar} \left[\frac{p^2}{2m} + \frac{\hbar\Omega}{4\Delta_{\mathrm{L}}} \cos^2 k_{\mathrm{L}} x, \tilde{\rho}_{\mathrm{gg}} \right] \quad.
\tag{2.40}
$$

This equation is simply the equation of motion for $\tilde{\rho}_{\mathrm{gg}}$ under the Hamiltonian

$$
H_{\tilde{\rho}} = \frac{p^2}{2m} + \frac{\hbar\Omega^2}{4\Delta_{\mathrm{L}}} \cos^2 k_{\mathrm{L}} x \quad,
\tag{2.41}
$$

which is equivalent to the Hamiltonian (2.34) when the zero-point of the potential is shifted. Notice that this adiabatic-elimination procedure is similar to the one commonly used to study laser cooling and trapping, where the excited state is eliminated, but spontaneous emission is not ignored; this procedure leads to a Fokker-Planck equation of motion for the atomic distribution [Stenholm86].

From this approach, it is clear that the adiabatic approximation is good after a time on the order of $1/\Gamma$, when the coherences have damped away. After this initial transient, the adiabatic approximation remains good as long as any modulations of the standing wave take place over a time long compared to $1/\Omega_{\mathrm{gen}}$. This is clear from the dressed-state result (2.26), because

such modulations will not excite transitions between the dressed states and thus cause the adiabatic approximation to break down. This argument thus sets limits on experiments where the lattice is pulsed, as in the atom-optical realization of the kicked rotor problem in Chapter 4.

2.5 Complications

Until this point we have argued that in the limit of large detuning Δ_L (compared to both the maximum Rabi frequency Ω and the atomic lifetime Γ), the motion of an atom in a standing wave of light is equivalent to a point particle moving conservatively in a sinusoidal potential. In this section we will discuss several ways in which the real atomic system differs from this idealized description.

2.5.1 Spontaneous Emission

In the parameter regime that we have discussed above, it is possible to use the results we have derived so far to estimate the rate of spontaneous emission due to the far-detuned light. From the form of the master equation (2.38), we see that the total rate of spontaneous emission is simply the product of the decay rate Γ and the excited-state population $\tilde{\rho}_{ee} = |\psi_e|^2$ (integrated over position). From Eq. (2.30), we have, after ignoring the momentum term,

$$|\psi_e|^2 = \frac{\Omega^2}{4\Delta_L^2} \cos^2 k_L x |\psi_g|^2 \quad . \tag{2.42}$$

Performing a spatial average and using $|\psi_g|^2 \simeq 1$, we find the scattering rate

$$R_{sc} = \frac{\Gamma \Omega^2}{8\Delta_L^2} \quad . \tag{2.43}$$

A more careful treatment of the spontaneous emission rate yields (see Appendix A)

$$R_{sc} = \frac{(\Gamma/2)\Omega^2 \cos^2 k_L x}{2(\Delta_L^2 + \Gamma^2/4) + \Omega^2 \cos^2 k_L x} \quad . \tag{2.44}$$

The momentum recoils from the emitted photons results in atomic momentum diffusion at the rate

$$D_{se} = \frac{\hbar^2 k_L^2 \Gamma \zeta^2}{4m} \frac{\Omega^2 \cos^2 k_L x}{2(\Delta_L^2 + \Gamma^2/4) + \Omega^2 \cos^2 k_L x} \quad , \tag{2.45}$$

where the kinetic energy diffusion coefficient D is defined such that $\langle p_x^2/(2m)\rangle$ grows asymptotically as Dt. Also, ζ^2 is the mean-square projection of the photon recoil along the direction of the standing wave (for radiation from a pure linearly oscillating dipole, $\zeta^2 = 2/5$; for light near the D_2 line of cesium, where the ground-state sublevels in either the $F_g = 3$ or the $F_g = 4$ manifold are uniformly populated, and the detuning Δ_L is large compared to the excited state hyperfine splittings, $\zeta^2 \approx 0.34$).

2.5.2 Stochastic Dipole Force

The dipole force on the atoms in the standing wave can also lead to momentum diffusion. The dipole moment of the atom fluctuates due to spontaneous emission, and this fluctuating dipole interacts with the field gradients in the standing wave to produce momentum diffusion at a rate [Gordon80; Balykin95]

$$
\begin{aligned}
D_{\text{sdf}} = {} & \frac{\hbar^2 k_L^2 \Gamma}{2m} \frac{\Omega^2 \sin^2 k_L x}{[2(\Delta_L^2 + \Gamma^2/4) + \Omega^2 \cos^2 k_L x]^3} \\
& \times \left[2\left(\Delta_L^2 + \frac{\Gamma^2}{4}\right)^2 + \left(\frac{3}{4}\Gamma^2 - \Delta_L^2\right)\Omega^2 \cos^2 k_L x + \frac{3}{2}\Omega^4 \cos^4 k_L x + \frac{\Omega^6}{\Gamma^2}\cos^6 k_L x \right] .
\end{aligned}
\tag{2.46}
$$

In writing down the diffusion rates (2.45) and (2.46), we have assumed nearly zero atomic velocity and ignored the velocity dependences of the diffusion rates [Balykin95].

2.5.3 Nonlinearities of the Potential

In Section 2.3, we saw how the center-of-mass potential

$$
V(x) = \frac{\hbar \Omega^2}{8\Delta_L} \cos 2k_L x
\tag{2.47}
$$

arises from the energy shift of the dressed states (to lowest order in Ω^2) and the assumption that the atom is in only one dressed state. Here we describe the corrections to this potential due to the nonlinear dependence of the dressed-state energies on Ω^2 as well as the mixed steady-state populations of the dressed states. The potential obtained from the optical Bloch equations is [Gordon80; Dalibard85; Balykin95]

$$
V(x) = \frac{\hbar \Delta_L}{2} \log\left(1 + \frac{\Omega^2}{2(\Delta_L^2 + \Gamma^2/4)}\cos^2 k_L x \right) .
\tag{2.48}
$$

Since we are primarily interested in the limit where Δ_{L} is large compared to both Γ and Ω, we can extract the first few Fourier components of (2.48),

$$V(x) = V_{02} \cos(2k_{\text{L}}x) + V_{04} \cos(4k_{\text{L}}x) + V_{06} \cos(6k_{\text{L}}x) + \ldots \quad , \tag{2.49}$$

where, if we define the (maximum) saturation parameter s as

$$s := \frac{\Omega^2}{2(\Delta_{\text{L}}^2 + \Gamma^2/4)} \quad , \tag{2.50}$$

we find

$$
\begin{aligned}
V_{02} &= (\hbar\Delta_{\text{L}}/2)\left[2 + 4\left(1 - \sqrt{1+s}\right)/s\right] \\
V_{04} &= (\hbar\Delta_{\text{L}}/2)\left[-(8 + 8s + s^2) + 4(2 + 3s + s^2)/\sqrt{1+s}\right]/s^2 \\
V_{06} &= (\hbar\Delta_{\text{L}}/2)\big[2(32 + 48s + 18s^2 + s^3) \\
&\qquad\qquad - 4(16 + 32s + 19s^2 + 3s^3)/\sqrt{1+s}\big]/(3s^3) \quad .
\end{aligned}
\tag{2.51}
$$

For small s, these become

$$
\begin{aligned}
V_{02} &= \frac{\hbar\Delta_{\text{L}}}{2}\left[\frac{1}{2}s - \frac{1}{4}s^2 + \frac{5}{32}s^3 - \frac{7}{64}s^4 + O(s^5)\right] \\
V_{04} &= \frac{\hbar\Delta_{\text{L}}}{2}\left[-\frac{1}{16}s^2 + \frac{1}{16}s^3 - \frac{7}{128}s^4 + O(s^5)\right] \\
V_{06} &= \frac{\hbar\Delta_{\text{L}}}{2}\left[\frac{1}{96}s^3 - \frac{1}{64}s^4 + O(s^5)\right] \quad .
\end{aligned}
\tag{2.52}
$$

Hence, the corrected potential to order Ω^4 is

$$V(x) = \left(\frac{\hbar\Omega^2}{8\Delta_{\text{L}}} - \frac{\hbar\Omega^4}{32\Delta_{\text{L}}^3}\right)\cos 2k_{\text{L}}x - \frac{\hbar\Omega^4}{128\Delta_{\text{L}}^3}\cos 4k_{\text{L}}x + O\left(\frac{\Omega^6}{\Delta^5}\right) \quad , \tag{2.53}$$

where we have ignored the Γ dependence in s. The Stark shift is due to stimulated Raman and Rayleigh transitions among the motional states of the atom induced by the field; since these corrections are higher order in Ω^2, we can associate them with higher-order photon processes.

2.5.4   Velocity Dependence

In addition to diffusive effects and the saturation of the light-induced potential, there are velocity-dependent forces associated with motion in the standing wave. If we assume small velocities ($k_{\text{L}}v \ll \Gamma$), then diabatic transitions between the dressed states are negligible, and the force to lowest order in v_x is [Gordon80; Balykin95; Dalibard85; Metcalf99]

$$\mathbf{F_v} = v_x \hat{x} 2\hbar\Delta_{\text{L}}k_{\text{L}}^2 \sin^2 k_{\text{L}}x \frac{\Gamma^2\Omega^2[2(\Delta_{\text{L}}^2 + \Gamma/4) - \Omega^2\cos^2 k_{\text{L}}x] - \Omega^6\cos^4 k_{\text{L}}x}{\Gamma[2(\Delta_{\text{L}}^2 + \Gamma^2/4) + \Omega^2\cos^2 k_{\text{L}}x]^3} \quad . \tag{2.54}$$

For small Ω^2, this force can be understood in terms of optical molasses, where Doppler shifts cause an imbalance of spontaneous scattering between the two beams (leading to a cooling force for red detunings) [Metcalf99]. For larger Ω^2, when the last term in (2.54) is dominant, this force can be understood in terms of the local steady-state dressed-level populations lagging behind the atomic position [Dalibard85]; furthermore, in this regime, the sign of the force is opposite to the weak-field case, so that a red detuning actually leads to a heating force.

2.5.5   Multilevel Structure of Cesium

The results that we have derived in this chapter have assumed a two-level electronic structure of the atom. The cesium D_2 line, however, is far more complicated than a two-level atom as a result of hyperfine structure (Appendix A). The ground state is split into two hyperfine levels, $F = 3$ and $F = 4$ (where F is the hyperfine quantum number), which are separated by 9.2 GHz. Each of these levels additionally has $2F + 1$ magnetic sublevels (which are degenerate in the absence of fields), labeled by the quantum number m_F. The excited state is split into four sublevels, $F = 2$, 3, 4, and 5, with splittings between adjacent levels around 200 MHz, each with a corresponding set of magnetic sublevels.

From this proliferation of states it is not at all obvious that the two-level model is appropriate. The first important step in simplifying this structure is that the atoms should be initially optically pumped into one of the ground state levels (but not necessarily into only one magnetic sublevel). Then the atoms are only coupled to three of the excited states due to angular momentum conservation (i.e., $F' = 2, 3$, or 4 are excited for atoms pumped into the $F = 3$ ground state manifold, and $F = 4$ atoms can be excited to $F' = 3, 4$, or 5). In the limit where the detuning Δ_L is large compared to the excited-state hyperfine splittings, the excited states can be regarded as degenerate. In this limit, and for a linearly polarized standing wave, a symmetry then applies, which makes the dipole moment independent of m_F, and it has the value 2.2×10^{-29} C $\cdot$ m (see Appendix A for details).

The detuning is not arbitrarily large, however, with the consequence that the effective lattice potential depth V_0 depends slightly on m_F [Mathur68]. This effect can be accounted for

by explicitly summing over the excited states to arrive at an effective dipole moment for each sublevel:

$$\frac{d_{\text{eff}}^2(m_F)}{\Delta_{\text{L}}} = \sum_{F'} \frac{|\langle F\ m_F|d_z|F'\ m_F\rangle|^2}{\Delta_{F'}} \quad . \tag{2.55}$$

Here, $\Delta_{F'}$ is the laser detuning from the $|F\ m_F\rangle \longrightarrow |F'\ m_F\rangle$ transition, and Δ_{L} is now the detuning with respect to an arbitrary reference point (since it drops out of the calculation of V_0). This dipole moment can then be used within the context of the two-level atom model.

2.5.6   Collisions

With experiments performed in a MOT, one obvious deviation from the single-atom picture is due to collisions between the atoms in the MOT cloud. We can give very rough estimates for the collision rate for the experimental conditions in a cesium MOT. The *s*-wave collision cross section for cesium atoms polarized in the $F = 4$, $m_F = 4$ state was measured to be 5×10^{-11} cm^2 at a temperature of 5 μK in [Arndt97]. Note that this cross section actually overestimates the situation in the unpolarized case. For the experiments in Chapter 4, the MOT density was 10^{11} cm^{-3}, and the mean velocity was around 3 cm/s for the initial condition. These values lead to an estimated collision probability of only 2%/ms. For the experiments in Chapter 6, the MOT density was much lower, around 10^8 cm^{-3}, as a result of velocity selection. After state preparation, the initial mean velocity was 0.8 cm/s, and thus the collision probability in this case was the much smaller 0.4%/s.

2.5.7   Experimental Values

To illustrate the magnitudes of the effects that we have discussed in this section, we calculate the values of these corrections (shown in Table 2.1) for several different sets of experimental parameters. The first set of parameters corresponds to the experiments in Chapter 4, where the optical lattice was pulsed to realize the kicked rotor. In these experiments, the lattice was pulsed on for $t_{\text{p}} = 300$ ns at a time; the maximum intensity used corresponds to a Rabi frequency of $\Omega/2\pi = 590$ MHz, and the lattice detuning was -6.1 GHz from the $F = 4 \longrightarrow F' = 5$ transition. The second set of parameters describes the chaos-assisted tunneling experiments

of Chapter 6, where the lattice amplitude was modulated as a $\cos^2$ function in time. A typical modulation period T here was 20 μs, the detuning was $\Delta_{\rm L}/2\pi = -50$ GHz and a typical (time-averaged) Rabi frequency used was $\Omega/2\pi = 110$ MHz. The third set of parameters also applies to the chaos-assisted tunneling experiments, but to the state-preparation phase where the atoms evolved in a somewhat deeper lattice ($\Omega/2\pi = 250$ MHz), but shorter time scales apply, since the atoms evolved in the full lattice for 6 μs (and for an additional 300 μs as the lattice was gradually ramped up from zero intensity). The design of an experiment necessarily entails many compromises, but we were able to keep the effects discussed here to a very acceptable minimum.

Table 2.1: Numerical values for the various effects described in Section 2.5. The three columns correspond to the three different experimental parameter regimes described in the text.

Parameter set	**Kicked Rotor**	**Tunneling**[1]	**Tunneling**[2]
$R_{\rm sc}$[3]	$1.1\%/t_{\rm p}$[4]	$0.040\%/T$[5]	$0.010\%/\mu$s
$D_{\rm sc}$[6]	$0.0039\,\hbar\omega_{\rm r}/t_{\rm p}$	$1.3 \times 10^{-4}\,\hbar\omega_{\rm r}/T$	$3.5 \times 10^{-5}\,\hbar\omega_{\rm r}/\mu$s
$D_{\rm sdf}$[7]	$0.012\,\hbar\omega_{\rm r}/t_{\rm p}$	$4.0 \times 10^{-4}\,\hbar\omega_{\rm r}/T$	$1.0 \times 10^{-4}\,\hbar\omega_{\rm r}/\mu$s
$|(V_{02} - V_0)/V_0|$[8]	0.23%	1.2×10^{-6}	6.3×10^{-6}
$|V_{04}/V_0|$[9]	0.058%	3.0×10^{-7}	1.6×10^{-6}
F_v[10]	$5.3 \times 10^{-8}\,\hbar k_{\rm L}/t_{\rm p}$	$-1.0 \times 10^{-11}\,\hbar k_{\rm L}/T$	$-2.7 \times 10^{-12}\,\hbar k_{\rm L}/\mu$s
$|\Delta V_0(m_F)/V_0(0)|$[11]	1.6%	0.11%	0.11%
Collision rate	$\sim 0.04\%/T$[12]	$\sim 8 \times 10^{-8}/T$	$\sim 4 \times 10^{-9}/\mu$s

[1] Modulated standing wave interaction portion of the chaos-assisted tunneling experiment.
[2] State-preparation portion of the chaos-assisted tunneling experiment.
[3] Spontaneous emission rate, averaged over a lattice period.
[4] The pulse width $t_{\rm p} = 300$ ns is the relevant time scale for the kicked-rotor experiment.
[5] $T = 20$ μs is a typical relevant time scale for the chaos-assisted tunneling experiment.
[6] Rate of diffusion due to spontaneous emission, averaged over a lattice period.
[7] Rate of diffusion due to stochastic dipole fluctuations, averaged over a lattice period.
[8] Correction to potential amplitude (relative to V_0).
[9] Amplitude of second harmonic potential component (relative to V_0).
[10] Velocity-dependent force, averaged over a lattice period for the recoil velocity ($v_{\rm r} = 3.5$ mm/s).
[11] Largest relative magnetic sublevel shift of V_0, normalized to the value for $m_F = 0$.
[12] The relevant time scale for this process is the $T = 20$ μs period of the potential.

2.6   Generalization to Two Nonidentical Traveling Waves

We now generalize the results derived so far to the case where the two traveling waves have different amplitudes and frequencies. In this case, the electric field is

$$
\begin{aligned}
\mathbf{E}(x,t) &= \hat{z}[E_{01}\cos(k_{\mathrm{L1}}x - \omega_{\mathrm{L1}}t) + E_{02}\cos(k_{\mathrm{L2}}x + \omega_{\mathrm{L2}}t)] \\
&= \hat{z}\Big(E_{01}\,e^{i(k_{\mathrm{L1}}x - \delta_{\mathrm{L}}t/2)} + E_{02}\,e^{-i(k_{\mathrm{L2}}x - \delta_{\mathrm{L}}t/2)}\Big)e^{-i\omega_{\mathrm{L}}t} + \text{c.c.} \\
&=: \mathbf{E}^{(-)}(x,t) + \text{c.c.} \ ,
\end{aligned}
\tag{2.56}
$$

where $\omega_{\mathrm{L}} := (\omega_{\mathrm{L1}} + \omega_{\mathrm{L2}})/2$ is the mean laser frequency, $\delta_{\mathrm{L}} := \omega_{\mathrm{L1}} - \omega_{\mathrm{L2}}$ is the frequency splitting between the two traveling waves, and we assume that $|\delta_{\mathrm{L}}| \ll |\Delta_{\mathrm{L}}|$, with $\Delta_{\mathrm{L}} := \omega_{\mathrm{L}} - \omega_0$. Then, in the rotating-wave approximation, the interaction Hamiltonian becomes

$$
\begin{aligned}
\tilde{H}_{\mathrm{AF}} &= -\tilde{\mathbf{d}}^{(+)}\cdot\tilde{\mathbf{E}}^{(+)} - \tilde{\mathbf{d}}^{(-)}\cdot\tilde{\mathbf{E}}^{(-)} \\
&= \frac{\hbar}{2}\Big(\Omega(x,t)a^{\dagger} + \Omega^{*}(x,t)a\Big) \ ,
\end{aligned}
\tag{2.57}
$$

where $\tilde{\mathbf{d}}$ and $\tilde{\mathbf{E}}$ are defined as before, and the time- and space-dependent Rabi frequency is defined by

$$
\Omega(x,t) := -\frac{\langle \mathrm{e}|d_z|\mathrm{g}\rangle}{\hbar}\left(E_{01}e^{i(k_{\mathrm{L1}}x - \delta_{\mathrm{L}}t/2)} + E_{02}e^{-i(k_{\mathrm{L2}}x - \delta_{\mathrm{L}}t/2)}\right) \ .
\tag{2.58}
$$

Writing out the Schrödinger equation yields the two coupled equations

$$
\begin{aligned}
i\hbar\partial_t\psi_{\mathrm{e}} &= \frac{p^2}{2m}\psi_{\mathrm{e}} + \frac{\hbar}{2}\Omega(x,t)\psi_{\mathrm{g}} - \hbar\Delta_{\mathrm{L}}\psi_{\mathrm{e}} \\
i\hbar\partial_t\psi_{\mathrm{g}} &= \frac{p^2}{2m}\psi_{\mathrm{g}} + \frac{\hbar}{2}\Omega^{*}(x,t)\psi_{\mathrm{e}} \ .
\end{aligned}
\tag{2.59}
$$

Making the adiabatic approximation gives the relation

$$
\hbar\Delta_{\mathrm{L}}\psi_{\mathrm{e}} = \frac{\hbar}{2}\Omega(x,t)\psi_{\mathrm{g}} \ ,
\tag{2.60}
$$

and hence yields the equation of motion for the ground-state amplitude,

$$
i\hbar\partial_t\psi_{\mathrm{g}} = \left(\frac{p^2}{2m}\right)\psi_{\mathrm{g}} + \frac{\hbar}{4\Delta_{\mathrm{L}}}|\Omega(x,t)|^2\psi_{\mathrm{g}} \ .
\tag{2.61}
$$

From Eq. (2.58), we find that

$$
\begin{aligned}
|\Omega(x,t)|^2 &= \frac{|\langle \mathrm{e}|d_z|\mathrm{g}\rangle|^2}{\hbar^2}\left|E_{01}e^{i(k_{\mathrm{L1}}x - \delta_{\mathrm{L}}t/2)} + E_{02}e^{-i(k_{\mathrm{L2}}x - \delta_{\mathrm{L}}t/2)}\right|^2 \\
&= \frac{|\langle \mathrm{e}|d_z|\mathrm{g}\rangle|^2}{\hbar^2}\Big[|E_{01}|^2 + |E_{02}|^2 + 2E_{01}E_{02}\cos(2k_{\mathrm{L}}x - \delta_{\mathrm{L}}t)\Big] \ ,
\end{aligned}
\tag{2.62}
$$

where $k_{\mathrm{L}} := (k_{\mathrm{L1}} + k_{\mathrm{L2}})/2$. Hence, we see that the atom obeys the center-of-mass Schrödinger equation $(i\hbar\partial_t\psi_{\mathrm{g}} = H\psi_{\mathrm{g}})$, where the Hamiltonian, after a potential offset has been subtracted, is given by

$$H = \frac{p^2}{2m} + V_0\cos(2k_{\mathrm{L}}x - \delta_{\mathrm{L}}t) \quad, \tag{2.63}$$

and

$$V_0 = \frac{|\langle\mathrm{e}|d_z|\mathrm{g}\rangle|^2 E_{01}E_{02}}{2\hbar\Delta_{\mathrm{L}}} \quad. \tag{2.64}$$

Thus, the motion is the same as before, except that the standing wave moves with velocity $\delta_{\mathrm{L}}/2k_{\mathrm{L}}$, and the potential depth is proportional to the geometric mean of the two traveling wave intensities. The velocity associated with the frequency difference is intuitive, as in a frame of reference moving with respect to an optical lattice, the two beams would be Doppler shifted in opposite senses, and would thus appear to have different frequencies.

2.7   Quantum Dynamics in a Stationary Standing Wave

Now that we have derived the equations of motion for an atom in an optical lattice, we will give an introduction to some aspects of the dynamics in the lattice that will be important in later chapters. Before continuing, though it is worth providing a set of scaled units in which to work. In order to simplify the Hamiltonian (2.34), we begin by noting that we have the freedom to independently rescale the coordinates to eliminate redundant parameters. There is a natural choice for the position scaling,

$$x' = 2k_{\mathrm{L}}x, \tag{2.65}$$

since the natural length scale is the $\lambda/2$ period of the standing-wave potential. In the pendulum, there is no explicit time scale that must be eliminated, so we are free to rescale such that Planck's constant is effectively unity. Thus, demanding that $[x', p'] = i$, we find that

$$p' = \frac{p}{2\hbar k_{\mathrm{L}}} \quad. \tag{2.66}$$

Using these scalings in the unscaled Hamiltonian (2.34), we find

$$H' = \frac{p'^2}{2} + \alpha_{\mathrm{p}}\cos x' \tag{2.67}$$

upon identifying $8\hbar\omega_r$ as the natural energy scale (recall that $\omega_r = \hbar k_L^2/2m$), so that $\alpha_p = V_0/(8\hbar\omega_r)$ and $H' = H/(8\hbar\omega_r)$. Notice that this energy scaling implies a time scaling of $t' = 8\omega_r t$, since we have already determined how action is scaled. In what follows we will drop the primes on the scaled units, and on occasion we will use unscaled units to emphasize particular points.

2.7.1 Bragg Scattering

The quantum-pendulum dynamics show a feature that is distinctly nonclassical: the momentum transferred from the potential to the atoms is quantized. To see this directly, we consider the Schrödinger equation in scaled units,

$$i\partial_t|\psi\rangle = \left(\frac{p^2}{2} + \alpha_p \cos x\right)|\psi\rangle \ . \tag{2.68}$$

In the momentum representation, where $\psi(p) := \langle p|\psi\rangle$, the Schrödinger equation can be rewritten as

$$i\partial_t\psi(p) = \frac{p^2}{2}\psi(p) + \frac{\alpha_p}{2}\left[\psi(p+1) + \psi(p-1)\right] \ . \tag{2.69}$$

This form follows from either recognizing $\exp(ikx)$ as a momentum-displacement operator, or by carrying out an explicit Fourier transform of the equation from the position to the momentum representation. So, the evolution in the standing wave imposes a "ladder" structure in momentum, such that an atom beginning in a plane-wave state $|p\rangle$ can only subsequently occupy the states $|p + n\rangle$ for integer n. In unscaled units, the quantization of the momentum is in multiples of $2\hbar k_L$, which has a clear interpretation in terms of the stimulated scattering of lattice photons: if the atom absorbs a photon that was traveling in one direction and then re-emits it into the counterpropagating mode, the atom will recoil, changing its momentum by twice the photon momentum, or by $2\hbar k_L$. Of course, the argument that we just considered was based on a classical treatment of the field, so it is the spatial periodicity of the potential that imposes the ladder structure in this model. However, as we will see in Chapter 5, the momentum transfer to the atoms can be viewed as a stimulated Raman transition between different motional states (say, $|p\rangle$ and $|p + 1\rangle$). The coupling between these two levels is described by a Raman Rabi

frequency (as in the two-level atom), given by

$$\Omega_{\mathrm{R}} = \frac{\Omega_1 \Omega_2}{2\Delta_{\mathrm{L}}} \quad , \tag{2.70}$$

where $\Omega_{1,2}$ are the Rabi frequencies associated separately with each traveling-wave component of the standing wave, and Δ_{L} is the mutual detuning to the atomic excited state (the relative frequency difference is constrained by energy conservation to be the splitting between the motional states). To connect with the notation that we have already used, $\Omega_1 = \Omega_2 = \Omega/2$ for the case of identical traveling waves, so that $\hbar\Omega_{\mathrm{R}} = V_0$, and thus V_0 also represents the strength of the Raman couplings.

The two-photon, stimulated Raman transition is an example of a *Bragg scattering* process [Martin88; Giltner95; Kozuma99]. In fact, it is the simplest ("first-order") form of Bragg scattering; in general, nth-order Bragg scattering is a $2n$-photon transition spanning an interval of $2n\hbar k_{\mathrm{L}}$ in momentum. The term "Bragg scattering" applies to the weakly coupled regime, where the intermediate states are not appreciably populated, and so the transition between the two distant momentum states can be treated as a two-level problem. In this regime, classical transport between these distinct momentum regions is forbidden, as the classical potential is not sufficiently strong to cause a correspondingly large change in the classical momentum. As such, Bragg scattering is an example of *dynamical tunneling*, which is quantum tunneling between re-
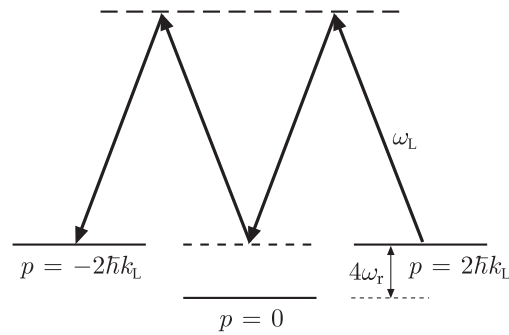

Figure 2.1: Level diagram for second-order Bragg scattering. This process occurs as a pair of two-photon Raman scattering processes, coupling the $2\hbar k_{\mathrm{L}}$ momentum level to the $-2\hbar k_{\mathrm{L}}$ level. The Bragg treatment is valid when the two-photon Rabi frequency Ω_{R} is small compared to the detuning $4\omega_{\mathrm{r}}$ from the intermediate state, which can then be adiabatically eliminated from the problem.

gions in phase space between which classical transport is forbidden, but by the dynamics (here, the nature of asymptotically free-particle motion) rather than by a potential barrier.

Although the potential has a small amplitude, quantum coherence can build up as the atoms sample the potential and cause the atoms to significantly change their motion. We will illustrate this process by considering the relatively simple case of second-order Bragg scattering, and then we will generalize our results to the nth-order case. We consider the case where the standing wave is stationary, so that only the states $|-2\hbar k_{\mathrm{L}}\rangle$ and $|2\hbar k_{\mathrm{L}}\rangle$ are resonantly coupled (we will stick to unscaled units for this derivation to emphasize the connection to the "quantum optics" view of the atomic motion) in the limit of small Ω_{R}. No other states will be substantially coupled by these fields, unless the Raman Rabi frequency is large enough to power-broaden the off-resonant transitions, which would not correspond to the Bragg regime. The relevant energy-level diagram is shown in Fig. 2.1, which shows that the detuning from the $|0\rangle$ motional state is simply the kinetic-energy shift. Neglecting couplings to other states (which are even further detuned than the $|0\rangle$ state), the Schrödinger equation for the three coupled momentum states then becomes

$$
\begin{aligned}
i\hbar\partial_t\psi(-2\hbar k_{\mathrm{L}},t) &= \frac{(2\hbar k_{\mathrm{L}})^2}{2m}\psi(-2\hbar k_{\mathrm{L}},t) + \frac{\hbar\Omega_{\mathrm{R}}}{2}\psi(0,t) \\
i\hbar\partial_t\psi(0,t) &= \frac{\hbar\Omega_{\mathrm{R}}}{2}\big[\psi(-2\hbar k_{\mathrm{L}},t) + \psi(2\hbar k_{\mathrm{L}},t)\big] \\
i\hbar\partial_t\psi(2\hbar k_{\mathrm{L}},t) &= \frac{(2\hbar k_{\mathrm{L}})^2}{2m}\psi(2\hbar k_{\mathrm{L}},t) + \frac{\hbar\Omega_{\mathrm{R}}}{2}\psi(0,t) \ .
\end{aligned}
\tag{2.71}
$$

Adding an energy offset of $-4\hbar\omega_{\mathrm{r}}$, the equations become

$$
\begin{aligned}
i\hbar\partial_t\psi(\pm 2\hbar k_{\mathrm{L}},t) &= \frac{\hbar\Omega_{\mathrm{R}}}{2}\psi(0,t) \\
i\hbar\partial_t\psi(0,t) &= \frac{\hbar\Omega_{\mathrm{R}}}{2}\big[\psi(-2\hbar k_{\mathrm{L}},t) + \psi(2\hbar k_{\mathrm{L}},t)\big] - 4\hbar\omega_{\mathrm{r}}\psi(0,t) \ .
\end{aligned}
\tag{2.72}
$$

Now we assume that $\Omega_{\mathrm{R}} \ll 4\omega_{\mathrm{r}}$, so that the population in the $|0\rangle$ state is $O(\Omega_{\mathrm{R}}^2/\omega_{\mathrm{r}}^2)$ and hence negligible. Additionally, we can make an adiabatic approximation for the evolution of the $|0\rangle$ state, by formally setting $\partial_t\psi(0,t) = 0$, as we did in Section 2.4. Again, though, this is a shortcut for considering the density-matrix picture and replacing the rapidly-varying coherences with their locally average value (although this procedure is a result of coarse-graining here, rather

than radiative damping as in the previous treatment). Doing so leads to the adiabatic relation

$$4\omega_\mathrm{r}\psi(0,t) = \frac{\Omega_\mathrm{R}}{2}\big[\psi(-2\hbar k_\mathrm{L},t) + \psi(2\hbar k_\mathrm{L},t)\big] \ , \tag{2.73}$$

which can be used to eliminate the intermediate state, resulting in a two-level evolution:

$$i\hbar\partial_t\psi(\pm 2\hbar k_\mathrm{L},t) = \frac{\hbar\Omega_\mathrm{R}^2}{16\omega_\mathrm{r}}\big[\psi(\pm 2\hbar k_\mathrm{L},t) + \psi(\mp 2\hbar k_\mathrm{L},t)\big] \ . \tag{2.74}$$

Hence the second-order Bragg Rabi frequency is $\Omega_{\mathrm{B},2} = \Omega_\mathrm{R}^2/8\omega_\mathrm{r}$. (The first term represents a Stark shift of $\Omega_{\mathrm{B},2}/2$, while the second term represents the Rabi-type coupling.) Comparing this expression to the form (2.70) for the two-photon Rabi frequency, we see that this second-order Bragg process can be viewed also as a Raman process of two Raman transitions, where the detuning to the intermediate state Δ_L is identified as $4\omega_\mathrm{r}$.

Continuing in this manner, the Bragg rate for nth-order scattering from $n\hbar k_\mathrm{L}$ to $-n\hbar k_\mathrm{L}$ is given by [Giltner95]

$$\Omega_{\mathrm{B},n} = \frac{\Omega_\mathrm{R}^n}{2^{n-1}\displaystyle\prod_{k=1}^{n-1}\delta_k} \ , \tag{2.75}$$

where δ_k is the detuning of the kth intermediate motional state. Notice that the intermediate detunings are given by $[n^2 - (n-2)^2]\omega_\mathrm{r}$, $[n^2 - (n-4)^2]\omega_\mathrm{r}$, ..., $[n^2 - (2-n)^2]\omega_\mathrm{r}$, so that this Bragg frequency can be written as

$$\Omega_{\mathrm{B},n} = \frac{\Omega_\mathrm{R}^n}{(8\omega_\mathrm{r})^{n-1}[(n-1)!]^2} \tag{2.76}$$

In scaled units, we can rewrite this frequency as

$$\Omega'_{\mathrm{B},n} = \frac{\alpha_\mathrm{p}^n}{[(n-1)!]^2} \ . \tag{2.77}$$

The transition frequency obviously becomes small for high-order Bragg processes, as the Rabi frequency decreases exponentially with the order. Nevertheless, Bragg oscillations of up to sixth [Giltner95] and eighth [Koolen00] order have been observed experimentally for an atomic beam crossing an optical standing wave.

2.7.2   Band Structure

As with any periodic potential, the eigenenergies for the atom in an optical lattice are grouped in bands, which are continuous intervals of allowed energies, separated by "band gaps" of forbidden energies. As this structure is relevant to some of the experiments performed in this dissertation,
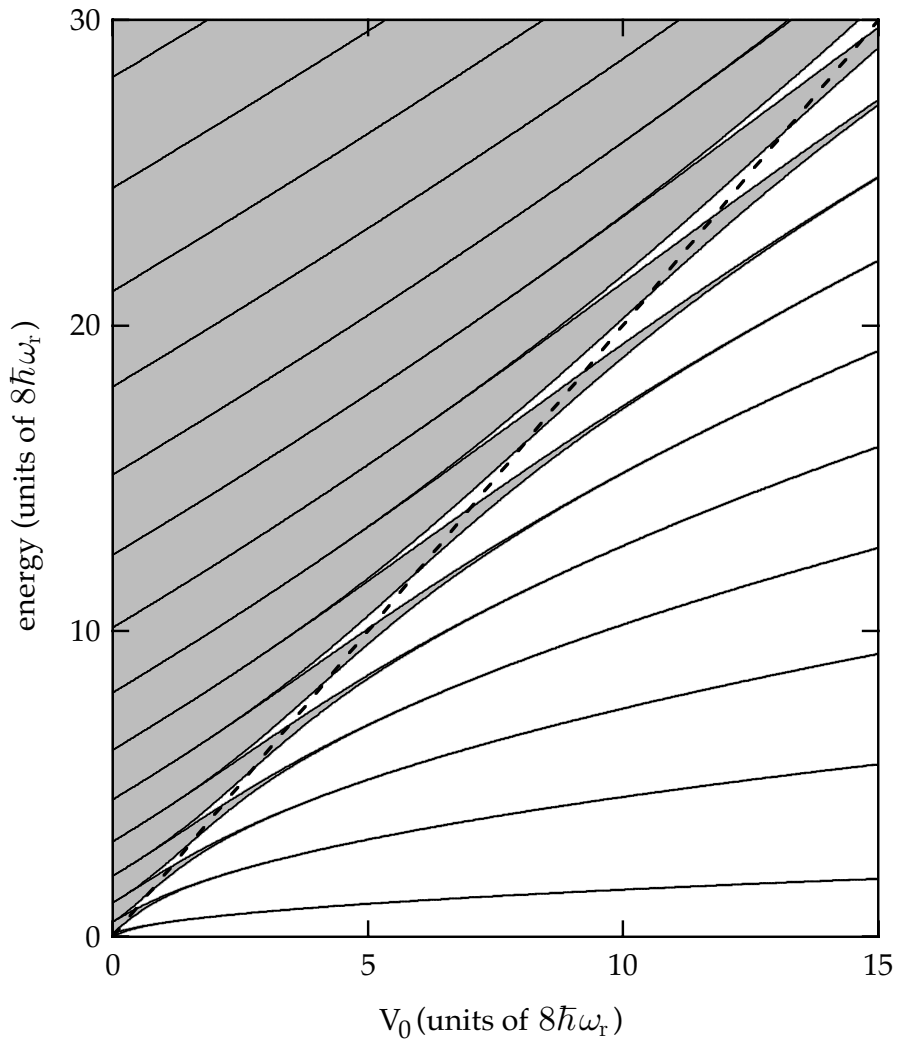

Figure 2.2: Plot of the allowed energy bands as a function of $V_0/8\hbar\omega_r$ (or equivalently α_p). The energies are also normalized to the natural unit scale $8\hbar\omega_r$, and are plotted relative to the potential minima. The shaded regions represent allowed energies, the solid lines represent the "edges" of the allowed bands, and the dashed line represents the energy of the peaks of the lattice.

we will treat this subject briefly. From Floquet's theorem (or equivalently, Bloch's theorem), the spatial periodicity of the time-independent Schrödinger equation for an atom in an optical lattice,

$$\left(\frac{p^2}{2} + \alpha_{\mathrm{p}} \cos x \right) \psi = E\psi \ , \tag{2.78}$$

implies that the solutions will be plane waves modulated by a periodic function,

$$\psi_q = e^{iqx} u_q(x), \tag{2.79}$$

where $u_q(x+2\pi) = u_q(x)$, and q is the "Floquet exponent" or "quasimomentum," which parameterizes the family of solutions. The eigenenergies and eigenfunctions can be computed using standard matrix-diagonalization methods to find solutions of the Mathieu equation [Leeb79; Shirts93a; Shirts93b]; the numerically calculated energy bands are plotted in Fig. 2.2 as a function of α_{p}. By convention, the quasimomentum is restricted to the range $[-1/2, 1/2)$, and the integer part n of the full quasimomentum is called the "band index." Note that solutions with
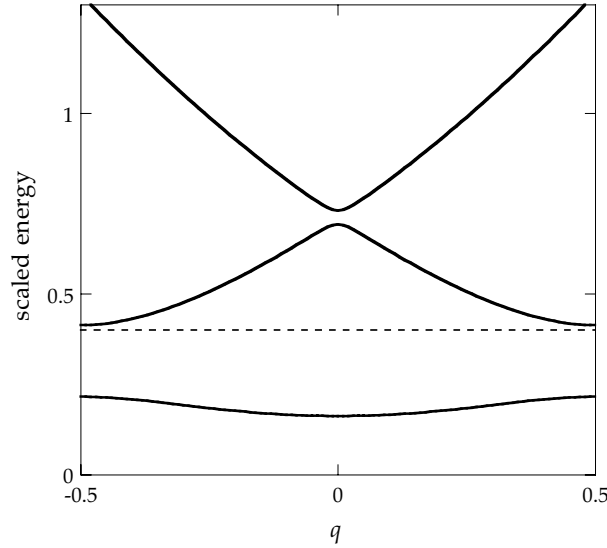

Figure 2.3: Plot of the lowest three energy bands for $\alpha_{\mathrm{p}} = V_0/8\hbar\omega_{\mathrm{r}} = 0.2$, where the band energy is plotted as a function of the quasimomentum q. This band structure is in the weakly coupled regime, where the lowest bands have significant curvature. The dashed line at the scaled energy of 0.4 marks the maximum potential energy of the lattice. The band gaps are a result of Bragg diffraction, which couples states with integer or half-integer quasimomentum and induces avoided crossings at these quasimomenta.

the same reduced quasimomentum q are similar in that they can be written in terms of plane-wave solutions with the same reduced quasimomentum:

$$\psi_{n,q} = \sum_{k=-\infty}^{\infty} c_{n,k} e^{i(k+q)x} \quad . \tag{2.80}$$

The energy bands are plotted as a function of the reduced quasimomentum for a small value of α_{p} in Fig. 2.3.

The band structure for small well depths can be understood in terms of Bragg scattering. In the free-particle case, the energy structure is that of a free particle, so that the energy is simply $q^2/2$, where we identify the quasimomentum with the real particle momentum. Bragg processes then couple certain degenerate pairs of the quasimomenta (the half-integer values), which are precisely the locations where the band gaps form. These band gaps can be viewed as avoided crossings of the energy as the quasimomentum varies. The avoided-crossing nature of the band gap is clear from the gaps plotted in Fig. 2.3, and the locations of the band gaps on the left edge of Fig. 2.2 are spaced according to n^2, as expected in the free-particle limit. As the bands make the transition to the deep-well limit (as in the right side of Fig. 2.2), they become narrow, as expected for trapped states. The band gaps becomes more uniform in size as well, as is expected for harmonic-oscillator states, which the lattice wave functions approach in the deep-well limit, when they only "see" the parabolic bottoms of the wells.

For our purposes there are two properties of the lattice wave functions that will be important. First, as long as the sinusoidal potential is the sole interaction potential for the atoms, the reduced quasimomentum is a constant of the motion, even if the lattice is temporally modulated. This property is simply a manifestation of the ladder structure that we already mentioned. The second property is that for slow changes of α_{p}, the band index is an adiabatic constant of the motion. This property is important in preparation of atomic states, because if the atoms can be cooled so that their momenta are within $(-\hbar k_{\mathrm{L}}, \hbar k_{\mathrm{L}})$ in free space, they will be loaded into the lowest energy band when the lattice is turned on adiabatically.

2.7.3 Boundary Conditions

Finally, we make a short comment on the nature of a "rotor" vs. a "particle," and the relevance of these ideas to optical-lattice experiments. A pendulum in the usual sense has an angle as a coordinate, and the coordinate space is equivalent to a 1-torus. In an extended realization of the pendulum, as in the optical lattice, the coordinate space is extended and formally equivalent to a line. The identification of the two situations comes from the periodicity of the potential in the extended case. Classically, there is no problem making this identification, since one can always take the extended coordinate modulo the period of the potential. Quantum mechanically, however, the boundary conditions in the two cases can lead to drastically different energy-level structures. Specifically, the periodic boundary condition in the case of the rotor implies that the spectrum is discrete, because only the integer quasimomentum states exist. In other words, the periodic boundary conditions pick out an obviously special class of states (the $q = 0$ "symmetric ladder," where each state is coupled to its degenerate partner via Bragg scattering) out of the possible continuum of ladders in the extended (particle) case. This difference has various consequences for atom-optics experiments, one of the most dramatic being that in Bragg scattering and chaos-assisted tunneling experiments, the transport only occurs for a relatively small set of states, which would naturally be selected in the case of a true rotor. In the case of dynamical localization as in Chapter 4, the localization still occurs in the particle case, although much of the theoretical analysis in the literature is for the rotor, which is obviously much simpler. Thus, despite this distinction, we will use the term "kicked rotor" to refer as well to the kicked particle.